発表者氏名	論文タイトル名	発表誌名	巻号	ページ	出版年
Sasaki-Suzuki N, Arai K, Ogata T, Kasahara K, Sakoda H, Chida K, **Asano T**, Pessin J F, Hakuno F, Takahashi SI.	GH inhibition of glucose uptake in adipocytes occurs without affecting GLUT4-translocation through an IRS-2-PI 3-kinase-dependent pathway.	J Biol Chem	284 (10)	6061-70	2009
Ikubo M, Wada T, Fukui K, Ishiki M, Ishihara H, **Asano T**, Tsuneki H, Sasaoka T.	Impact of lipid phosphatases SHIP2 and PTEN on the time- and Akt isoform-specific amelioration of TNF{alpha}-induced insulin resistance in 3T3-L1 adipocytes.	Am J Physiol Endocrinol Metab	296	E157-64	2009
Cui X, Kushiyama A, Yoneda M, Nakatsu Y, Guo Y, Zhang J, Ono H, Kanna M, Sakoda H, Ono H, Kikuchi T, Fujishiro M, Shiomi M, Kamata H, Kurihara H, Kikuchi M, Kawazu S, Nishimura F, **Asano T**.	Macrophage foam cell formation is augmented in serum from patients with diabetic angiopathy.	Diabetes Res Clin Pract	87(1)	57-63	2010
Yoneda M, Guo Y, Ono H, Nakatsu Y, Zhang J, Cui X, Iwashita M, Kumamoto S, Tsuchiya Y, Sakoda H, Fujishiro M, Kushiyama A, Koketsu Y, Kikuchi T, Kamata H, Nishimura F, **Asano T**.	Decreased SIRT1 expression and LKB1 phosphorylation occurs with long-term high-fat diet feeding, in addition to AMPK phosphorylation impairment in the early phase.	Obesity Res Clin Pract			in press

Psychiatry and Clinical Neurosciences 2009; 63: 65–72 doi:10.1111/j.1440-1819.2008.01889.x

Regular Article

Neuropathy is associated with depression independently of health-related quality of life in Japanese patients with diabetes

Sumiko Yoshida, MD, PhD,[1]* Masashi Hirai, MD, PhD,[2] Susumu Suzuki, MD, PhD,[2] Shuichi Awata, MD, PhD[3] and Yoshitomo Oka, MD, PhD[2]

[1]*Department Psychiatry, Faculty of Medicine, Saitama Medical University, Saitama,* [2]*Division of Molecular Metabolism and Diabetes, Tohoku University Graduate School of Medicine, and* [3]*Department of Psychiatry, Tohoku University Graduate School of Medicine, Sendai, Japan*

Objectives: To identify factors independently associated with depression in Japanese patients with diabetes, after controlling for potential confounding factors.

Methods: Among 197 outpatients with diabetes, 129 (type 1: 24, type 2: 105) completed a questionnaire concerning socio-demographic and health-related variables. Depression screening was done using Zung's Self-Rating Depression Scale test, followed by diagnostic interviews by experienced psychiatrists employing the Diagnostic Statistical Manual of Mental Disorders, 4th edition (DSM-IV).

Results: Forty-seven patients (36.4%) had symptomatological depression. A Self-Rating Depression Scale cut-off score of 40 had good sensitivity (100%) and modest specificity (59%) for detecting major depressive episode, in accordance with the DSM-IV. Diabetic patients suffering from depression were more likely to have neuropathy, retinopathy, body pain, a feeling of poor general health, and lack of social support, than the non-depressed patients. However, age, gender, marital status, diabetes type, insulin requirement, duration of diabetes, hemoglobin A1c (HbA1c) and the presence of nephropathy did not differ between the two groups. In multivariate logistic regression analysis, body pain (OR 3.26, 95% CI 1.31–8.08) and the presence of microvascular complications (OR 2.81, 95% CI 1.13–6.98) were independent factors associated with depression. Specifically, diabetic neuropathy (OR 3.10, 95% CI 1.17–8.22) was associated with depression independently of age, gender, marital status, social supports, quality of life, diabetes type, duration of diabetes, HbA1c, and insulin requirement.

Conclusions: A diabetic complication, specifically neuropathy, was independently associated with depression in patients with diabetes. The present findings indicate the need to find a biological base common to both depression in diabetes and diabetic neuropathy.

Key words: depression, diabetes, mental health, neuropathy, quality of life

DEPRESSION IS MORE common among diabetic patients in western countries. Recent studies have documented a doubling of depression rates in individuals with, as compared to those without, diabetes.[1,2] It has been shown that diabetic patients who are depressed have poorer glycemic control,[3] are less physically active,[4] and more obese.[5] Depression appears to be a very important problem in the management of diabetes.

**Correspondence: Sumiko Yoshida, MD, PhD, Deptartment Psychiatry, Faculty of Medicine, Saitama Medical University, Moroyama-machi, Iruma, Saitama 350-0495, Japan. Email: yoshidas@saitama-med.ac.jp*

Address of the institution at which the work was carried out: Div. Molecular Metabolism and Diabetes, Tohoku Univ. Grad. Sch. Med., Sendai, 980-8575, Japan

Received 11 February 2008; revised 13 September 2008; accepted 14 September 2008.

To date, the socio-demographic factors reported to be associated with depression include: female gender,[2] younger age,[2,6] being unmarried,[2,7,8] lower levels of education[6,8] and lack of social support.[9] Factors concerning health-related quality of life (QOL), such as perception of poor general health[10] and body pain,[11] were also associated with depression. Poor glycemic control,[3,7] types of diabetes treatment,[8] duration of diabetes,[8] presence of diabetic complications,[8,12] diabetic neuropathy[13–15] and retinopathy[9,16] were similarly associated with depression. However, these reports did not adequately control for potential confounding factors. Are there any factors underlying both depression and diabetes?

The prevalence of major depressive episodes in the Japanese diabetic population according to the Diagnostic Statistical Manual of Mental Disorders 4th edition (DSM-IV),[17] has not been investigated. In addition, only a few studies designed to identify factors associated with depression in individuals with diabetes in Asian countries, including Japan, have been reported. We first investigated the prevalence of depression, diagnosed by experienced psychiatrists, to confirm the increased prevalence of major depressive episodes in Japanese diabetic patients. Then we investigated factors possibly associated with depression in diabetic patients using multivariate logistic analysis, after controlling for the potential confounding factors.

METHODS

Subjects

All 197 patients who visited the Diabetes and Metabolism Unit, Tohoku University Hospital in November 2003 were recruited. The diagnosis of type 1 or type 2 diabetes had been made in accordance with the criteria of the American Diabetes Association.[18] One hundred twenty-nine of the 197 patients (65%) completed a questionnaire concerning socio-demographic and health-related variables. This study was conducted under the guidelines of the ethics committee at the Tohoku University. The procedures were fully explained to each subject before the assessments and written informed consent was obtained from each subject.

Measurement

Gender, age, marital status, the number of family members, educational level, and social support were assessed as socio-demographic variables. For social support, one item was selected from among the five items used in previous Japanese studies[19,20] as the strongest association with depression was found in the present samples. Health-related quality of life was assessed using the subscales for pain and perception of general health in the Japanese version of the Short-Form 36 Health Survey questionnaire.[21,22] All scores were dichotomized by the average score of the Japanese general population.

Diabetes type (Types 1 and 2), duration of illness (≧10 and <10 years), body mass index (BMI), medical regimen, anti-hypertensive requirements, hypolipidemic requirements, and blood pressure were obtained from the patient's medical record. Fasting plasma glucose concentration, hemoglobin A1c (HbA1c, ≧7 and <7%), and plasma lipid levels (Triglycerides [TG], total cholesterol [TC], high density lipoprotein cholesterol [HDL], and low density lipoprotein cholesterol [LDL]) were also evaluated as variables representing glycemic control status.

Microvascular complications were defined as the presence of at least one of the following: diabetic nephropathy, neuropathy or retinopathy. Diabetic nephropathy was defined as the presence of persistent proteinuria. Diabetic neuropathy was defined as the presence of symmetric neuropathic symptoms in the lower extremities and/or absence of bilateral Achilles tendon reflexes. Diabetic retinopathy, diagnosed by experienced ophthalmologists, was categorized as: simple, preproliferative or proliferative retinopathy, or none.

Assessment of depression

The Zung Self-Rating Depression Scale (SDS)[23] was used to screen for depression. Patients scoring 40 or more on the SDS were defined as suffering from depression.[24,25] The Japanese version of the SDS has been extensively validated.[26] All patients with a score of 40 or more on the SDS were suggested to undergo a psychiatric evaluation using the DSM-IV to diagnose a possible major depressive episode within the following one-month period. Almost the same number of patients with scores under 40 on the SDS had the same interviews as the controls. None of the subjects who were interviewed were taking any psychoactive drugs during the study.

Statistical analysis

The χ^2 test or *t*-test was used to compare differences in characteristics between diabetic patients with and without depression. Multivariate logistic regression analysis was used to estimate the association between depression and potential predictor variables by calculating odds ratios (OR) and 95% confidence intervals (95% CI). All statistical analyses were performed using SPSS for Windows, version 11.5J. A value of $P < 0.05$ was considered to be statistically significant.

RESULTS

Prevalence of depression and major depressive episode

Forty- seven out of 129 subjects (36.4%) had depression. Thirty-one of the 47 depressed subjects underwent diagnostic interviewing by experienced psychiatrists. Seven (type 1: 3, type 2: 4) of these 31 were diagnosed as having a major depressive episode. None of 34 subjects with SDS scores below 40, who had the same interviews, were diagnosed as having a major depressive episode. (Fig. 1 shows the experimental design.) Thus, the prevalence of a current major depressive episode in adult diabetic patients was estimated to be 7.9%. There is no difference of the prevalence between type 1 and type 2 ($P = 0.34$). In this study, an SDS cut-off of 40 yielded good sensitivity (100%) and modest specificity (59%) for detecting a major depressive episode in accordance with the DSM-IV.

Comparison of characteristics of diabetic patients with and without depression

The characteristics of patients with and without depression are presented in Table 1. The depressed

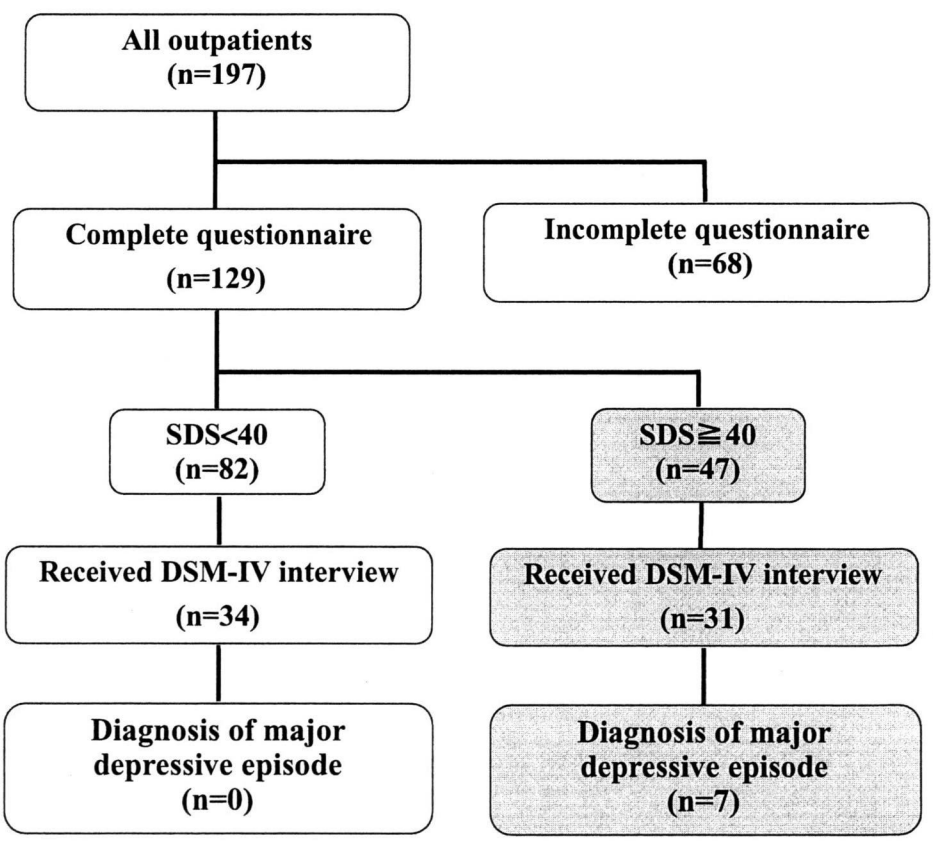

Figure 1. Experimental design. SDS, Zung Self-Rating Depression Scale; DSM-IV, Diagnostic Statistical Manual of Mental Disorders, 4th edition.

Table 1. Characteristics of patients with and without depression

Variables	SDS < 40 ($n = 82$)	SDS ≧ 40 ($n = 47$)
Gender		
Female	35	23
Male	47	24
Age	54.12 ± 10.31	52.72 ± 10.47
Martial status		
Married	66	32
Unmarried	16	15
Number of family members	3.13 ± 1.45	3.32 ± 1.80
Social support		
+	77	38
–	5	9*
SF36: pain	76.72 ± 23.80	63.24 ± 27.00**
SF36: general health	54.82 ± 18.00	40.93 ± 22.91**
Education		
~ junior high school	9	4
~ high school	42	33
~ college (university)	31	10
Diabetes type		
Type 1	13	11
Type 2	69	36
Duration of illness		
<10 years	53	24
≧10 years	29	23
BMI (kg/M^2)	24.07 ± 4.69	24.07 ± 3.74
Insulin		
+	45	27
–	37	20
Anti-hypertensive agent		
+	25	12
–	57	35
Hypolipidemic agent		
+	27	9
–	55	38
Blood pressure (mmHg)	127.6 ± 15.0	126.3 ± 15.8
Diastolic	77.4 ± 10.1	75.0 ± 8.8
Systolic	146.61 ± 38.20	154.04 ± 66.90
Fasting blood glucose (mg/dl)	7.00 ± 1.19	7.12 ± 1.69
HbA1c (%)	112.76 ± 59.93	118.57 ± 73.70
TG (mg/dl)	193.82 ± 28.90	193.60 ± 35.99
TC (mg/dl)	56.40 ± 19.84	52.60 ± 17.25
HDL (mg/dl)	113.57 ± 26.10	117.40 ± 30.83
LDL (mg/dl)		
Microvascular complications		
+	28	28**
–	54	19
Nephropathy		
+	12	5
–	70	42
Neuropathy		
+	14	18**
–	68	29
Retinopathy		
+	19	20*
–	63	27

Data are means ± SD or N. BMI, body mass index; HbA1c, hemoglobin A1c; HDL, high density lipoprotein cholesterol; LDL, low density lipoprotein cholesterol; SDS, Zung Self-Rating Depression Scale; SF36, Short-Form 36 Health Survey questionnaires, TC, total cholesterol; TG, triglycerides; persons without pain have higher pain scores, persons who perceive themselves as having good health have higher scores for general health. *$P < 0.05$; **$P < 0.01$ by t-test or χ^2 test.

patients were more likely to lack social support ($P < 0.05$), have pain (P. 0.01), and feel that their general health was poor ($P < 0.01$), than patients without depression. The prevalence of microvascular complications, that is, diabetic neuropathy and/or retinopathy, was also higher in the patients with than in those without depression ($P < 0.01$). In contrast, age, gender, marital status and educational level did not differ between the two groups. There was also no difference in the diabetes type, duration of diabetes, BMI, insulin requirement, blood pressure, antihypertensive medication requirement, fasting plasma glucose concentration, HbA1c, plasma lipid levels, hypolipidemic medication requirement or the presence of nephropathy between the depressed and non-depressed patients.

Multivariate analysis

Tables 2 and 3 show the factors predictably associated with depression in diabetic patients. As shown in Table 2, the subjective feeling of body pain (OR = 3.26, 95% CI = 1.31–8.08) and the presence of microvascular complications (OR = 2.81, 95% CI = 1.13–6.98) were independently associated with depression. In the analysis focused on neuropathy rather than the presence of microvascular complications in general, the presence of diabetic neuropathy (OR = 3.10, 95% CI = 1.17–8.22) was significantly associated with depression (Table 3). This association was independent of age, gender, marital status, social support, pain, a perception of poor general health, diabetes type, duration of diabetes, HbA1c, and insulin requirement. Neither nephropathy nor retinopathy was independently associated with depression.

Table 2. Factors independently associated with depression: with respect to microvascular complications

Independent variables	OR	95% CI	p
Age	0.99	0.95–1.03	0.76
Gender			
Male	1.00		
Female	1.10	0.47–2.58	0.83
Marital status			
Married	1.00		
Unmarried	1.55	0.60–4.01	0.37
Social support			
+	1.00		
–	2.04	0.68–8.55	0.17
SF 36: pain			
≧76.2	1.00		
<76.2	3.26	1.31–8.08	0.011*
SF 36: general health			
≧65.0	1.00		
<65.0	1.34	0.47–3.80	0.58
Type of diabetes			
Type 2	1.00		
Type 1	2.02	0.68–5.98	0.21
Duration of diabetes (years)			
<10	1.00		
≧10	1.75	0.74–3.92	0.21
HbA1c (%)			
<7.0	1.00		
≧7.0	0.56	0.23–1.37	0.20
Insulin			
–	1.00		
+	0.76	0.28–2.02	0.58
Microvascular complication			
–	1.00		
+	2.81	1.13–6.98	0.026*

*$P < 0.05$ by multivariate logistic regression analysis.
65.0, mean score on the general health subscale of the SF36 in the Japanese population (persons who perceive themselves as having good health have higher scores); 76.2, mean score on the pain subscale of the SF36 in the Japanese population (persons without pain have higher scores); 95% CI, 95% confidence intervals; HbA1c, hemoglobin A1c; OR, odds ratio; SF36: Short-Form 36 Health Survey questionnaire.

DISCUSSION

The prevalence of a DSM-IV major depressive episode in adult diabetic patients was estimate to be 7.9%, that is, higher than that of the general Japanese population (1%; DSM-III)[27] or working population (4%; ICD-10).[28] The prevalence range for current depression, diagnosed by structured diagnostic interviews of diabetic patients, was reported to be 11.0–19.9% in uncontrolled studies.[29] The prevalence determined in this study was lower than those reported previously. It might partially be explained by the fact that 16 out of 47 depressive patients who seemed to have severed depressive symptoms refused to be psychiatrically interviewed. However, our result confirmed an increased prevalence of a major depressive episode in diabetic patients as compared to the general population not only in Western countries but also in Japan.

Our findings on the characteristics of patients with and without depression are partially consistent with the results of earlier studies on the relationship

Table 3. Factors independently associated with depression: with respect to neuropathy

Independent variables	OR	95% CI	*P*
Age	1.00	0.95–1.04	0.83
Gender			
Male	1.00		
Female	1.04	0.45–2.43	0.93
Marital status			
Married	1.00		
Unmarried	1.74	0.67–4.51	0.26
Social support			
+	1.00		
–	2.64	0.76–9.22	0.13
SF 36: pain			
≧76.2	1.00		
<76.2	3.53	1.42–8.81	0.007**
SF 36: general health			
≧65.0	1.00		
<65.0	1.25	0.44–3.50	0.68
Type of diabetes			
Type 2	1.00		
Type 1	1.96	0.66–5.77	0.23
Duration of diabetes (years)			
≧10	1.71		
<10	1.00	0.75–3.93	0.21
HbA1c (%)			
<7.0	1.00		
≧7.0	0.57	0.23–1.41	0.22
Insulin			
–	1.00		
+	0.78	0.30–2.11	0.64
Neuropathy			
–	1.00		
+	3.10	1.17–8.22	0.023*

*$P < 0.05$; **$P < 0.01$ by multivariate logistic regression analysis.

65.0, mean score on the general health subscale of the SF36 in the Japanese population (persons who perceive themselves as having good health have higher scores); 76.2, mean score on the pain subscale of the SF36 in the Japanese population (persons without pain have higher scores); 95% CI, 95% confidence intervals; HbA1c, hemoglobin A1c; OR, odds ratio; SF36, Short-Form 36 Health Survey questionnaire.

between diabetes and depression. Relationships between lack of social support,[9] perception of poor general health[10] or body pain[11] and depression in diabetic patients have been reported previously. Similarly, the presence of microvascular complications,[8,12] specifically neuropathy[13–15] and retinopathy,[9,16] are related to depression. However, our results do not support a relationship between depression and the following factors; female gender,[2] younger age,[2,6] being unmarried,[2,7] lower levels of education,[6,8] poor glycemic control,[3,7] types of diabetes treatment[8] and duration of diabetes.[8] The discrepancies across studies might be attributable, at least in part, to differences in patient characteristics. The patients in our study had essentially adequate glycemic control (HbA1c: 7.0 ± 1.4, FBS: 149 ± 50) at the start of the study and most had attained a high level of education. Thus, glycemic control status and educational level appear not to be related to depression.

In multivariate logistic regression analysis, the presence of microvascular complications, specifically neuropathy, was associated with depression independently of age, gender, marital status, social support, pain, perception of general health, diabetes type, duration of diabetes, HbA1c, and insulin requirement. Diabetic complications decreased health-related QOL, which is associated with increased risk of psychological impairment.[30,31] One of the subscales for health-related QOL, body pain, was also reported to be strongly associated with depression.[11,13] It was also suggested that individuals with inadequate support are most at risk of becoming depressed when disability related to illness increased.[31] Thus, several previous reports suggested depression in diabetic patients to be secondarily induced by decreased health-related QOL and/or inadequate social support. However, our results demonstrate that depression is not necessarily secondarily induced by pre-existing factors because a diabetic complication, specifically neuropathy, was independently associated with depression regardless of health-related QOL and/or social support.

There is a possibility that diabetic microvascular impairment induces both neuropathy[32] and so-called vascular depression[33] in diabetic patients. However, it seems unlikely that depression in diabetic patients would be vascular in origin because neither nephropathy nor retinopathy was independently associated with depression in this study.

The present findings indicate the need to find a biological base common to both depression in diabetes and diabetic neuropathy.

However, there are limitations to interpreting the results of this study. First, because this analysis is based on cross-sectional data, causality can not be determined. Prospective studies are needed. Second, this study has sample size limitation. Future studies

enrolling adequate samples of diabetic patients are required.

CONCLUSION

Diagnostic interviews, conducted by experienced psychiatrists, demonstrated a higher prevalence of current major depressive episodes (7.9%) in Japanese diabetic patients than in the general population. Multivariate logistic regression analyses demonstrated neuropathy to be an independent factor associated with depression in diabetic patients.

ACKNOWLEDGMENTS

This work was supported by a Grant-in-Aid for Research on the Human Genome, Tissue Engineering (H17-genome-003) from the Ministry of Health, Labour and Welfare of Japan to Y. O.

REFERENCES

[1] Anderson RJ, Freedland KE, Clouse RE, Lustman PJ. The prevalence of comorbid depression in adults with diabetes: A meta-analysis. *Diabetes Care* 2001; 24: 1069–1078.

[2] Egede LE, Zheng D, Simpson K. Comorbid depression is associated with increased health care use and expenditures in individuals with diabetes. *Diabetes Care* 2002; 25: 464–470.

[3] Lustman PJ, Anderson RJ, Freedland KE, de Groot M, Carney RM, Clouse RE. Depression and poor glycemic control: A meta-analytic review of the literature. *Diabetes Care* 2000; 23: 934–942.

[4] Caruso LB, Silliman RA, Demissie S, Greenfield S, Wagner EH. What can we do to improve physical function in older persons with type 2 diabetes? *J. Gerontol. A Biol. Sci. Med. Sci.* 2000; 55: M372–M377.

[5] Katon W, von Kroff M, Ciechanowski P *et al.* Behavioral and clinical factors associated with depression among persons with diabetes. *Diabetes Care* 2004; 27: 914–920.

[6] Peyrot M, Rubin RR. Persistence of depressive symptoms in diabetic adults. *Diabetes Care* 1999; 22: 448–452.

[7] Hanninen JA, Takala JK, Keinanen-Kiukaanniemi SM. Depression in subjects with type 2 diabetes. Predictive factors and relation to quality of life. *Diabetes Care* 1999; 22: 997–998.

[8] Peyrot M, Rubin RR. Levels and risks of depression and anxiety symptomatology among diabetic adults. *Diabetes Care* 1997; 20: 585–590.

[9] Miyaoka Y, Miyaoka H, Motomiya T, Kitamura S, Asai M. Impact of sociodemographic and diabetes-related characteristics on depressive state among non-insulin-dependent diabetic patients. *Psychiatry Clin. Neurosci.* 1997; 51: 203–206.

[10] Jacobson AM, de Groot M, Samson JA. The effects of psychiatric disorders and symptoms on quality of life in patients with type I and type II diabetes mellitus. *Qual. Life Res.* 1997; 6: 11–20.

[11] Bair MJ, Robinson RL, Katon W, Kroenke K. Depression and pain comorbidity: A literature review. *Arch. Intern. Med.* 2003; 163: 2433–2445.

[12] Padgett DK. Sociodemographic and disease-related correlates of depressive morbidity among diabetic patients in Zagreb, Croatia. *J. Nerv. Ment. Dis.* 1993; 181: 123–129.

[13] Takahashi Y, Hirata Y. A follow-up study of painful diabetic neuropathy: Physical and psychological aspects. *Tohoku J. Exp. Med.* 1983; 141: 463–471.

[14] Winocour PH, Main CJ, Medlicott G, Anderson DC. A psychometric evaluation of adult patients with type 1 (insulin-dependent) diabetes mellitus: Prevalence of psychological dysfunction and relationship to demographic variables, metabolic control and complications. *Diabetes Res.* 1990; 14: 171–176.

[15] Viinamäki H, Niskanen L, Uusitupa M. Mental well-being in people with non-insulin-dependent diabetes. *Acta Psychiatr. Scand.* 1995; 92: 392–397.

[16] Black SA. Increased health burden associated with comorbid depression in older diabetic Mexican Americans. Results from the Hispanic Established Population for the Epidemiologic Study of the Elderly survey. *Diabetes Care* 1999; 22: 56–64.

[17] American Psychiatric Association. *Diagnostic and Statistical Manual of Mental Disorders*, 4th edn. American Psychiatric Association, Washington, DC, 1994.

[18] The expert committee on the diagnosis and classification of diabetes mellitus. Report of the expert committee on the diagnosis and classification of diabetes mellitus. *Diabetes Care* 1997; 20: 1183–1197.

[19] Muraoka Y, Oiji A, Ihara K. The physical, psychological and social background factors of elderly depression in the community (in Japanese). *Jpn. J. Geriatr. Psychiatry* 1996; 7: 397–407.

[20] Koizumi Y, Awata S, Seki T *et al.* Association between social support and depression in the elderly Japanese population (in Japanese with English abstract). *Nippon Ronen Igakkai Zasshi* 2004; 41: 426–433.

[21] Fukuhara S, Bito S, Green J, Hsiao A, Kurokawa K. Translation, adaptation, and validation of the SF-36 Health Survey for use in Japan. *J. Clin. Epidemiol.* 1998; 51: 1037–1044.

[22] Fukuhara S, Ware JE Jr, Kosinski M, Wada S, Gandek B. Psychometric and clinical tests of validity of the Japanese SF-36 Health Survey. *J. Clin. Epidemiol.* 1998; 51: 1045–1053.

[23] Zung WA. Self-rating depression scale. *Arch. Gen. Psychiatry* 1965; 12: 63–70.

[24] Zung WWK. A cross-cultural survey of symptoms in depression. *Am. J. Psychiatry* 1969; 126: 116–121.

[25] Barrett J, Hurst MW, DiScala C, Rose RM. Prevalence of depression over a 12-month period in a non-patient population. *Arch. Gen. Psychiatry* 1978; **35**: 741–744.
[26] Fukuda K, Kobayashi S. A study on a self-rating depression scale. *Psychiatr. Neurol. Jpn.* 1978; **75**: 673–679.
[27] Fujihara S, Kitamura T. Psychiatric epidemiologic research in an area of Kofu city: The prevalence of mild psychiatric disorder using JCM diagnosis (in Japanese). *Nippon Iji Shinpou* 1992; **3618**: 47–50.
[28] Kawakami N, Iwata N, Tanigawa T *et al.* Prevalence of mood and anxiety disorders in a working population in Japan. *J. Occup. Environ. Med.* 1996; **38**: 899–905.
[29] Gavard JA, Lustman PJ, Clouse RE. Prevalence of depression in adults with diabetes. An epidemiological evaluation. *Diabetes Care* 1993; **16**: 1167–1178.
[30] Jacobson AM, Rand LI, Hauser ST. Psychologic stress and glycemic control: A comparison of patients with and without proliferative diabetic retinopathy. *Psychosom. Med.* 1985; **47**: 327–381.
[31] Littlefield CH, Rodin GM, Murray MA, Craven JL. Influence of functional impairment and social support on depressive symptoms in persons with diabetes. *Health Psychol.* 1990; **9**: 737–749.
[32] Low PA. Recent advances in the pathogenesis of diabetic neuropathy. *Muscle Nerve* 1987; **10**: 121–128.
[33] Alexopoulos GS, Meyers BS, Young RC, Campbell S, Silbersweig D, Charlson M. 'Vascular depression' hypothesis. *Arch. Gen. Psychiatry* 1997; **54**: 915–922.

ORIGINAL ARTICLE

DOC2B: A Novel Syntaxin-4 Binding Protein Mediating Insulin-Regulated GLUT4 Vesicle Fusion in Adipocytes

Naofumi Fukuda,[1] Masahiro Emoto,[1] Yoshitaka Nakamori,[1] Akihiko Taguchi,[1] Sachiko Miyamoto,[1] Shinsuke Uraki,[1] Yoshitomo Oka,[2] and Yukio Tanizawa[1]

OBJECTIVE—Insulin stimulates glucose uptake in skeletal muscle and adipose tissues primarily by stimulating the translocation of vesicles containing a facilitative glucose transporter, GLUT4, from intracellular compartments to the plasma membrane. The formation of stable soluble *N*-ethyl-maleimide–sensitive fusion protein [NSF] attachment protein receptor (SNARE) complexes between vesicle-associated membrane protein-2 (VAMP-2) and syntaxin-4 initiates GLUT4 vesicle docking and fusion processes. Additional factors such as munc18c and tomosyn were reported to be negative regulators of the SNARE complex assembly involved in GLUT4 vesicle fusion. However, despite numerous investigations, the positive regulators have not been adequately clarified.

RESEARCH DESIGN AND METHODS—We determined the intracellular localization of DOC2b by confocal immunofluorescent microscopy in 3T3-L1 adipocytes. Interaction between DOC2b and syntaxin-4 was assessed by the yeast two-hybrid screening system, immunoprecipitation, and in vitro glutathione S-transferase (GST) pull-down experiments. Cell surface externalization of GLUT4 and glucose uptake were measured in the cells expressing DOC2b constructs or silencing DOC2b.

RESULTS—Herein, we show that DOC2b, a SNARE-related protein containing double C2 domains but lacking a transmembrane region, is translocated to the plasma membrane upon insulin stimulation and directly associates with syntaxin-4 in an intracellular Ca^{2+}-dependent manner. Furthermore, this process is essential for triggering GLUT4 vesicle fusion. Expression of DOC2b in cultured adipocytes enhanced, while expression of the Ca^{2+}-interacting domain mutant DCO2b or knockdown of DOC2b inhibited, insulin-stimulated glucose uptake.

CONCLUSIONS—These findings indicate that DOC2b is a positive SNARE regulator for GLUT4 vesicle fusion and mediates insulin-stimulated glucose transport in adipocytes. ***Diabetes* 58: 377–384, 2009**

Insulin stimulates glucose uptake in skeletal muscles and adipose tissues primarily by stimulating the translocation of vesicles containing a facilitative glucose transporter, GLUT4, from intracellular compartments to the plasma membrane (1,2). In addition to this translocation step, membrane fusion processes are also controlled by insulin (3,4). Like other regulated exocytotic processes in many cell types, the formation of stable soluble *N*-ethyl-maleimide–sensitive fusion protein [NSF] attachment protein receptor (SNARE) complexes between vesicle-associated membrane protein-2 (VAMP-2) and syntaxin-4 initiates GLUT4 vesicle docking and fusion processes (5). However, the precise mechanism by which insulin regulates SNARE complex assembly remains poorly understood.

In neurons, Ca^{2+} triggers exocytotic membrane fusion of synaptic vesicles to the plasma membrane, and calcium sensor proteins such as synaptotagmins have critical roles in this process (6,7). Similar mechanisms result in GLUT4 vesicle fusion in adipocytes and muscle cells. Whitehead et al. (8) demonstrated, and we confirmed, that reduction of intracellular Ca^{2+} ($[Ca^{2+}]_i$) using the membrane-permeable Ca^{2+}-chelating agent BAPTA-AM diminished insulin-stimulated glucose transport, whereas this reagent did not inhibit GLUT4 translocation to the plasma membrane (i.e., GLUT4 vesicle trafficking was not impaired) (8) (N.F., M.E., unpublished observation). These observations suggest that an appropriate intracellular Ca^{2+} level may be required for the final docking/fusion steps of GLUT4 vesicles in adipocytes.

The universal role of Ca^{2+} as a trigger for regulated exocytosis predicts the existence of conserved proteins capable of activating the fusion machinery upon binding Ca^{2+}. Although many proteins have been suggested to play such a role, synaptotagmins have attracted the most attention as putative calcium sensor proteins functioning in regulated exocytosis (9). Synaptotagmin family proteins have tandem C2 domains at the C-terminus. These two domains, C2A and C2B, are conserved in all 13 synaptotagmins described to date and constitute Ca^{2+}-binding modules (10). Many proteins have been identified as being involved in the GLUT4 vesicle fusion machinery in adipocytes. However, neither synaptotagmins nor other calcium sensor proteins have as yet been reported to regulate GLUT4 vesicle fusion.

We investigated, in detail, the mechanisms of Ca^{2+}-dependent GLUT4 vesicle fusion in adipocytes. We searched for double C2 domain proteins as candidate Ca^{2+} sensor proteins suitable for the relatively slow (on the order of several minutes) SNARE complex formation, and we found that DOC2b bound syntaxin-4 upon insulin stimulation in an intracellular Ca^{2+}-dependent manner and

From the [1]Division of Endocrinology, Metabolism, Hematological Sciences, and Therapeutics, Department of Bio-Signal Analysis, Yamaguchi University Graduate School of Medicine, Ube, Japan; and the [2]Division of Molecular Metabolism and Diabetes, Tohoku University Graduate School of Medicine, Sendai, Japan.

Corresponding author: Dr. Masahiro Emoto, emotom@yamaguchi-u.ac.jp.

Received 3 March 2008 and accepted 17 November 2008.

Published ahead of print at http://diabetes.diabetesjournals.org on 25 November 2008. DOI: 10.2337/db08-0303.

Additional information for this article can be found in an online appendix at: http://dx.doi.org/10.2337/db08-0303.

mediated GLUT4 vesicle fusion. DOC2b may be a downstream target of the insulin signal and a positive regulator of SNARE assembly involving regulated exocytosis in adipocytes.

RESEARCH DESIGN AND METHODS

Mouse DOC2a and DOC2b cDNA constructs were kindly provided by Dr. R.R. Duncan (University of Edinburgh, Edinburgh, U.K.). Mouse munc18c cDNA construct was kindly provided by Dr. T. Takuma (School of Dentistry, Health Sciences University of Hokkaido, Hokkaido, Japan).

Cell culture. 3T3-L1 fibroblasts were grown in Dulbecco's modified Eagle's medium (DMEM) with 10% fetal bovine serum (FBS) at 37°C. The cells (3–5 days after confluence) differentiated into adipocytes with incubation in the same DMEM, containing 0.5 mmol/l isobutylmethylxanthine, 0.25 μmol/l dexamethasone, and 4 μg/ml insulin, for 3 days and were then grown in DMEM with 10% FBS for an additional 5–8 days.

Plasmids and antibodies. Wild-type DOC2b was subcloned into peGFP-C2, pDsRed2-C1 (Clontech, Palo Alto, CA), and pGEX-6P1 (GH Healthcare, Buckinghamshire, U.K.) vectors. Calcium interacting domain mutants (CIMs) of DOC2b (D157N, D163N, D297N, and D303N) were subcloned into peGFP-C2 and pGEX-6P1 vectors. We also constructed syntaxin-4 and a series of deletion mutants of DOC2b corresponding to Δmunc13 interaction domain (MID) (amino acids 36–413), ΔC2A (2–120 and 252–413), and ΔC2B (2–264) in a peGFP-C2 vector. Myc-tagged DOC2b (wild-type or CIM) was subcloned into a pcDNA3 vector. All chemically synthesized and PCR-derived DNA sequences were verified by DNA sequencing.

Rabbit polyclonal DOC2b antibody was generated against the peptide sequence CGARDDDEDVDQL specific for DOC2b isoform. This antibody was found to cross-react minimally (online appendix Fig. S1 [available at http://dx.doi.org/10.2337/db08-0303). The following antibodies were used: monoclonal anti-GLUT4 (clone 1F8) (R&D systems, Minneapolis, MN), polyclonal anti-GLUT4, anti-GST (Santa Cruz Biotechnology, Santa Cruz, CA), anti-myc (clone 9E10) (Covance, Princeton, NJ), polyclonal anti–syntaxin-4 (Synaptic Systems, Gottingen, Germany), and fluorescent-conjugated and horseradish peroxidase–conjugated secondary antibodies (Jackson Immuno Research, West Grove, PA).

DOC2b shRNA construct. Short-hairpin RNA (shRNA) specific for mouse DOC2b was designed to have a 5′-GCCAGATGTAGACAAGAAATC-3′ sequence. Synthetic complementary single-stranded DNA of the target sequence was annealed, and the double-stranded DNA was inserted into a pcPUR+U6i cassette (11). This shRNA decreased DOC2b protein expression to 10–20% of the control level within 74 h. A same cassette encoding nonspecific scramble sequence was used as a negative control.

Preparation of recombinant adenovirus vectors. Adenovirus producing enhanced green fluorescent protein (eGFP), myc-tagged DOC2b (wild type, CIM mutant), and shRNA (DOC2b, control) were prepared using an AdEasy adenovirus vector system according to the manufacturer's instructions (Stratagene, Cedar Creek, TX). All amplified viruses were purified by the cesium chloride centrifugation method and stored at −80°C.

Live cell imaging of DOC2b. The peGFP-DOC2b was electroporated into 3T3-L1 adipocytes, which were then reseeded onto 0.1-mm glass-bottom dishes (Matsunami, Tokyo, Japan). At 24–48 h after electroporation, cells were serum starved for 3–4 h in DMEM and then incubated at 37°C for 2 h in Krebs-Ringer HEPES buffer (130 mmol/l NaCl, 5 mmol/l KCl, 1.3 mmol/l $CaCl_2$, 1.3 mmol/l $MgSO_4$, 25 mmol/l HEPES [pH 7.4]). The cells were treated with 100 nmol/l of insulin at 37°C for the time indicated and observed by laser confocal microscopy (LSM510 Pascal; Carl Zeiss, Oberkochen, Germany). For the translocation analysis, fluorescent intensities at three distinct areas in plasma membrane, cytosol, and nucleus (nine areas per cell each) of three independent cells were analyzed by Photoshop software CS2.

Yeast two-hybrid screening. The Matchmaker Yeast Two-Hybrid System (Clontech) was used for determination of DOC2b-binding partners. Full-length DOC2b and munc18c cDNA were subcloned into a pLexA vector and full-length syntaxin-4 and munc18c cDNA into a pB42AD vector. A standard lithium acetate/single-stranded carrier DNA/polyethylene glycol method for transformation into yeast strain EGY48 (p8op-lacZ) was used, and these proteins were expressed in this strain. Transcriptional activation of LacZ was determined by an X-Gal assay. β-Galactosidase activity was detected within 16 h of reaction at 30°C.

In vitro GST pull-down assay. Glutathione S-transferase (GST) fusion proteins of wild-type and CIM DOC2b were purified according to the manufacturer's instructions. GST syntaxin-4 was cleaved with PreScission Protease (2 units/μl) (GH Healthcare) in buffer containing 50 mmol/l Tris-HCl (pH 7.0), 150 mmol/l NaCl, 1 mmol/l EDTA, and 1 mmol/l dithiothreitol at 4°C for 16 h. At the end of incubation, cleaved syntaxin-4 protein was further purified using Amicon Ultra filter devices (Millipore, Danvers, MA).

Recombinant individual GST-DOC2bs or GST (1 μg each) were incubated with 1 μg of recombinant syntaxin-4 in 1 ml of Tris-buffered saline (20 mmol/l Tris, pH 7.4, 150 mmol/l NaCl) plus 0.5% Triton X-100 in the presence of 2 mmol/l EDTA or 1 mmol/l $CaCl_2$ for 4–6 h. This mixture was immunoprecipitated by incubating with Glutathion Sepharose 4B (GE Healthcare) for 1 h. The precipitates were washed four times and analyzed by SDS-PAGE and immunoblotting. Approximately 5% of syntaxin-4 was pulled down by the GST-DOC2b.

Northern blotting. Total RNAs were prepared from 3T3-L1 fibroblasts, 3T3-L1 adipocytes (days 3 and 9 of differentiation) or rat epididymal fat, and mouse brain using ISOGEN (Nippongene, Tokyo, Japan) and denatured in formaldehyde/formamide, resolved by electrophoresis, and transferred to hybond-N membranes (GH Healthcare). The membranes were hybridized with α-[^{32}P]–labeled full-length DOC2a and DOC2b cDNAs as probes and then washed three times with 1× saline sodium citrate buffer (15 mmol/l NaCl, 15 mmol/l sodium citrate [pH 7.0], and 0.1% SDS) at 65°C. Radioisotopic measurements were conducted using a Phosphorimager FLA2000 (Fuji film, Tokyo, Japan).

Immunoprecipitation and immunoblotting. A 10-cm plate of cells was lysed in 1 ml of lysis buffer (20 mmol/l HEPES [pH 7.2], 100 mmol/l NaCl, 25 mmol/l NaF, 1 mmol/l sodium vanadate, 1 mmol/l benzamidine, 5 μg/ml leupeptin, 5 μg/ml aprotinin, 1 mmol/l phenylmethylsulphonyl fluoride, 1 mmol/l dithiothreitol, and 0.5% NP-40) in the presence of 2 mmol/l EDTA or 1 mmol/l $CaCl_2$ and centrifuged for 15 min at 15,000*g*. The postnuclear lysates were used for the following experiments. The protein concentration was measured with a bicinchoninic acid protein assay reagent (Pierce, IL). For immunoprecipitation, the cell lysates were preincubated with protein-G/A–Sepharose at 4°C for 30 min to remove nonspecific bound proteins. Then, samples were incubated with primary antibodies at 4°C for 8–12 h followed by incubation with protein-G/A–Sepharose. Lysates and immunoprecipitates were resolved by SDS-PAGE and transferred to a polyvinylidene fluoride membrane (GH Healthcare). The membranes were incubated with primary antibodies for 8–12 h. Protein signals were visualized using horseradish peroxidase–conjugated secondary antibodies and an enhanced chemiluminescence substrate kit (GH Healthcare). The efficiencies of immunoprecipitation of the associated protein in Fig. 3*C–E* were ~1, 0.5, and 0.6%, respectively. All the images in figures are representative, and we repeated the immunoblots at least three times and found similar results.

Immunofluorescence microscopy and digital image analysis. Differentiated 3T3-L1 adipocytes were left untreated or electroporated by eGFP-DOC2b (wild type, CIM, ΔMID, ΔC2A, and ΔC2B), eGFP alone, DsRed2-DOC2b (wild type, CIM), shRNAs (control, DOC2b), or myc-GLUT4-eGFP. The cells were then replated onto coverslips and allowed to recover for 48 h. Cells were preincubated in the presence or absence of 50 μmol/l of BAPTA-AM for 10 min, followed by incubation with or without insulin for 20 min at 37°C. Next, the cells were fixed with 3.7% formaldehyde in PBS and permeabilized with buffer A (0.5% Triton X-100, 1% FBS in PBS) for 15 min. For the detection of endogenous proteins, the coverslips were incubated for 2 h with primary antibodies at room temperature. The cells were washed and incubated with an appropriate secondary antibody for 30 min. The coverslips were washed thoroughly again and mounted on glass slides. Immunostained cells were observed at room temperature with an LSM 5 PASCAL laser-scanning confocal microscope and its two-channel–scanning module (Carl Zeiss) equipped with an inverted Zeiss Axiovert 200M using the 63× oil objective lens (numerical aperture 1.4) run by LSM 5 processing software and Adobe Photoshop CS2. At least five cells were observed in a condition. The experiments were repeated at least three times, unless stated otherwise. All the images in figures are representative, and the conclusions are based on qualitative visual impression. The cell surface myc-GLUT4-eGFP was measured by subtracting the internal myc signal from total myc signal of electroporated cells. The plasma membrane eGFP content was also measured. The cell surface GLUT4 was calculated as (total myc − internal myc)/(total eGFP − internal eGFP) (22).

2-Deoxy-glucose uptake. Differentiated adipocytes were prepared in 24-well plates. Cells were infected with the recombinant adenoviruses. Two days thereafter, the cells were serum starved for 2 h at 37°C in Krebs-Ringer HEPES buffer. Then, the cells were stimulated with or without 100 nmol/l of insulin for 10 min, and 2-deoxy-glucose uptake was determined by 2-deoxy-D-[2,6 ^{3}H] glucose incorporation. Nonspecific glucose uptake was measured in the presence of 20 μmol/l cytochalasin B and subtracted from each determination to obtain specific uptake. The results were normalized by the protein amount.

Statistical analysis. Multiple comparisons among groups were performed using one-way ANOVA (post hoc test: Tukey-Kramer). Results are presented as means ± SD. Values of $P < 0.05$ were considered statistically significant.

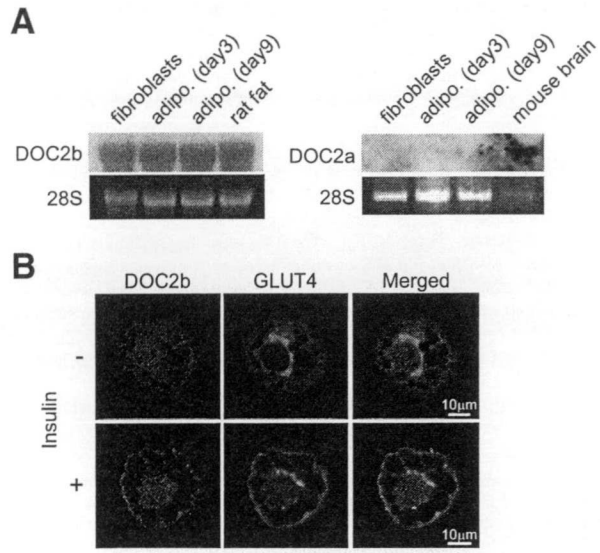

FIG. 1. **The expression profiles and intracellular localization of DOC2b in 3T3-L1 adipocytes. *A*: The expressions of DOC2a and DOC2b in 3T3-L1 fibroblasts, 3T3-L1 adipocytes (days 3 and 9 of differentiation), rat epididymal fat, and mouse brain were analyzed by mRNA blot. *B*: Differentiated 3T3-L1 adipocytes were serum-starved for 3–4 h and then stimulated with 100 nmol/l of insulin for 20 min, fixed, and immunostained. The endogenous DOC2b and GLUT4 were visualized using anti-DOC2b and anti-GLUT4 antibodies and observed by confocal microscopy. (Please see http://dx.doi.org/10.2337/db08-0303 for a high-quality digital representation of this figure.)**

RESULTS

DOC2b translocates to the plasma membrane in response to insulin. Type C tandem C2 domain proteins are classified into three groups (i.e., synaptotagmin and synaptotagmin-like protein and DOC2 family proteins). The first two groups of proteins regulate relatively fast membrane fusion (on the order of milliseconds to a few seconds) (12,13). This time scale is not suitable for GLUT4 vesicle fusion. Therefore, we focused on DOC2 family proteins as candidate regulators of GLUT4 vesicle fusion. First, we determined the expression profile of DOC2 mRNA in adipocytes. As shown in Fig. 1*A*, DOC2a was not expressed in 3T3-L1 adipocytes. According to a previous study, DOC2γ is localized to the nucleus and has no Ca^{2+}-binding activity because of amino acid substitutions at the Ca^{2+}-binding sites (14). Thus, we investigated the function of the DOC2b isoform involved in GLUT4 membrane fusion. Next, we examined the intracellular localization of DOC2b in differentiated 3T3-L1 adipocytes using anti-DOC2b antibody (Fig. 1*B*) or by expressing an eGFP fused to DOC2b (Fig. 2*A*). As shown in Fig. 1*B*, DOC2b results in a fine punctate or granular appearance throughout the cytoplasm under basal conditions. In contrast, the addition of insulin yields relatively slow (~5 min) translocation of DOC2b to the cell periphery (Fig. 2*A*). This time scale of translocation was very similar to that of GLUT4 vesicles. It is noteworthy that deletion of the MID enhanced plasma membrane localization even in the absence of insulin and that the C2B domain is necessary for membrane targeting (Fig. 2*B*). These observations are interesting in considering the distinct roles of the C2A and C2B domains and the negative regulatory function of MID. We performed additional experiments to determine the role of calcium in the translocation of DOC2b. As shown in Fig. 2*C*, the cell membrane permeable Ca^{2+}-chelating

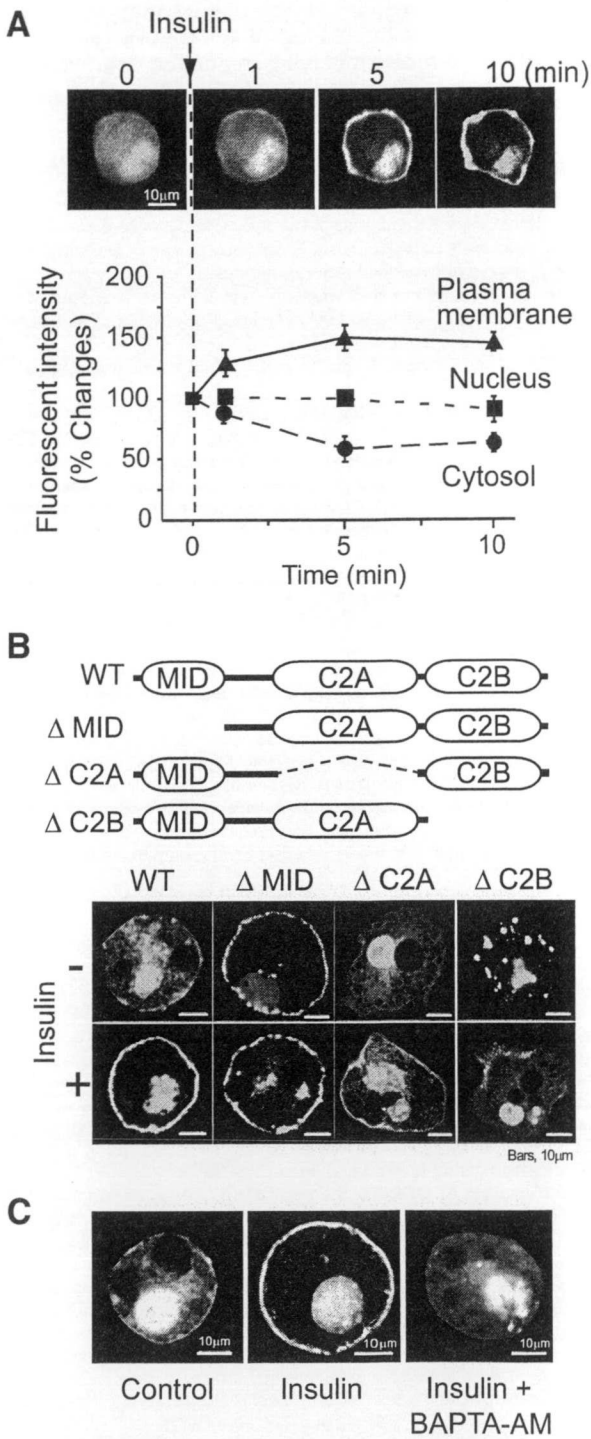

FIG. 2. **Insulin augments DOC2b translocation to the plasma membrane. *A*: 3T3-L1 adipocytes were electroporated with eGFP-DOC2b and then treated with 100 nmol/l of insulin for the times indicated. Live fluorescent images of the cells were captured by confocal microscopy. Relative fluorescences of the plasma membrane, nucleus, and cytosol were each measured in three distinct areas. At least three cells were analyzed for each condition. Results are means ± SD from three independent experiments. *B*: 3T3-L1 adipocytes expressing eGFP-DOC2b (WT [wild type], ΔMID, ΔC2A, or ΔC2B) were treated with or without 100 nmol/l of insulin and observed by confocal microscopy. *C*: 3T3-L1 adipocytes were electroporated with eGFP-DOC2b and then pretreated with 50 μmol/l of BAPTA-AM for 10 min, before treatment with insulin and observed under a confocal microscope.**

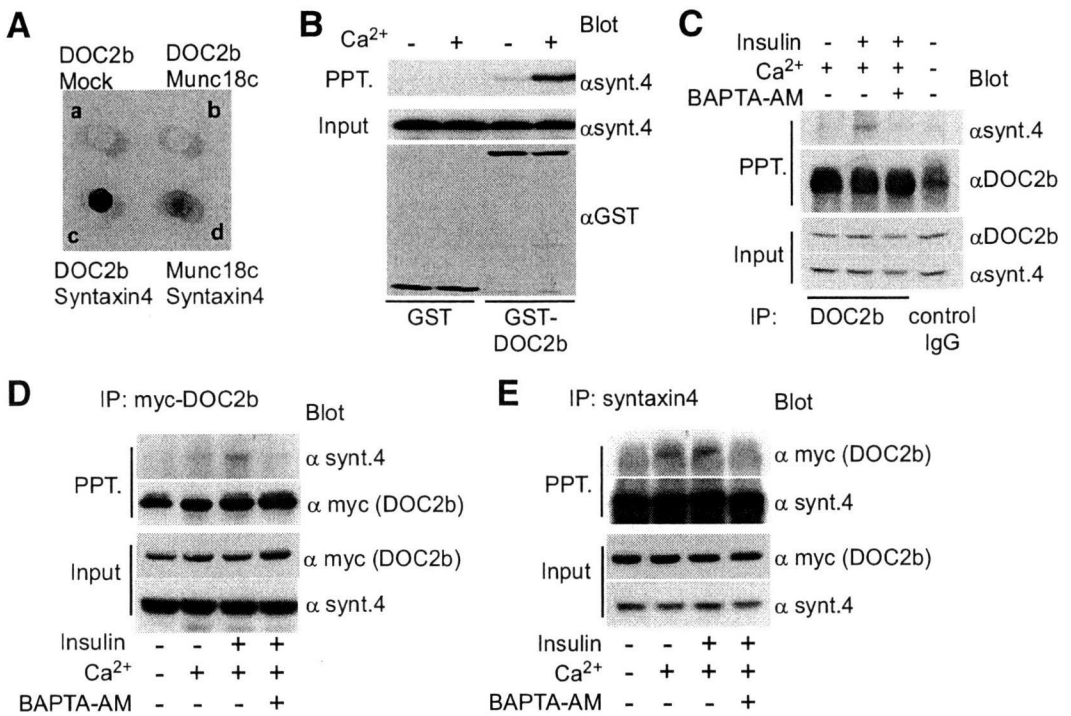

FIG. 3. Insulin promotes Ca^{2+}-dependent interaction between DOC2b and syntaxin-4. *A*: pLexA containing DOC2b or munc18c and pB42AD containing munc18c, syntaxin-4 (synt.4) or empty vectors were coexpressed in the yeast strain of EGY48 (p8op-lacZ), followed by incubation at 30°C for 16 h. Transcriptional activation of LacZ was determined by β-galactosidase assay. *B*: GST-tagged DOC2b and syntaxin-4 were bacterially expressed. Syntaxin-4 protein was cleaved by PreScession protease and further purified with Amicon Ultra filter devices. Both proteins (1 μg each) were mixed in Tris-buffered saline in the presence of 2 mmol/l EDTA or 1 mmol/l $CaCl_2$ and pulled down by glutathione sepharose. The precipitates were analyzed by Western blotting with anti–syntaxin-4 and anti-GST antibodies. *C*: 3T3-L1 adipocytes were serum-starved for 3–4 h and pretreated with or without 50 μmol/l of BAPTA-AM before insulin treatment. The DOC2b–syntaxin-4 interaction was determined by immunoprecipitation using anti-DOC2b antibody. The immunoprecipitated proteins were immunoblotted with anti–syntaxin-4 and anti-DOC2b antibodies. *D* and *E*: Myc-tagged DOC2b was expressed by adenovirus vector in 3T3-L1 adipocytes. After serum starvation and pretreatment with or without 50 μmol/l of BAPTA-AM, before insulin treatment, the cells were stimulated with or without 100 nmol/l of insulin for 20 min and then immunoprecipitated with anti-myc or anti–syntaxin-4 antibodies. The immunoprecipitated proteins were immunoblotted with anti-myc and anti–syntaxin-4 antibodies.

agent BAPTA-AM inhibited insulin-dependent translocation of DOC2b.

DOC2b binds syntaxin-4 upon stimulation with insulin. Since DOC2b is thought to be a soluble calcium-sensing protein, compartment-specific targeting must be achieved through interaction with membrane-bound proteins such as SNARE and SNARE-related proteins. Therefore, we attempted to identify DOC2b-binding partners among these proteins using a yeast two-hybrid system. We found a very strong interaction between DOC2b and syntaxin-4 compared with the already known binding between munc18c and syntaxin4 (Fig. 3*A*). Interestingly, this t-SNARE protein is reportedly a key molecule for GLUT4 vesicle fusion in response to insulin (5,15). Although this interaction was very strong, SNARE proteins are quite "sticky" and can on occasion bind with many proteins nonspecifically. Therefore, we performed the following three additional experiments. First, we determined the direct interaction in vitro using recombinant proteins, GST-tagged DOC2b, and synthesized syntaxin-4. As shown in Fig. 3*B*, the interaction was easily detected by immunoblotting in the presence of calcium. Second, we examined endogenous protein-protein interactions by immunoprecipitation experiments using polyclonal anti-DOC2b. As shown in Fig. 3*C*, insulin treatment increased DOC2b–syntaxin-4 binding, and BAPTA-AM abolished this interaction. Since the molecular weights of DOC2b and the IgG heavy chain are quite similar (computed molecular weight of DOC2b and syntaxin-4 are 46 and 34 kDa, respectively), it was difficult to perform a reverse immunoprecipitation experiment. Third, our results were confirmed by immunoprecipitation experiments using adipocytes expressing myc-tagged DOC2b (Fig. 3*D* and *E*). It is important to note that we could not detect the interaction between DOC2b and syntaxin-4 in the buffer containing EDTA (data not shown). Furthermore, we could not find interaction between DOC2b and syntaxin6 in 3T3-L1 adipocytes (online appendix Fig. S2).

To better assess the calcium dependency of DOC2b translocation and interaction with syntaxin-4 in adipocytes, we conducted the following additional experiments using a Ca^{2+}-unbound mutant. Based on the information from crystallographic analysis of synaptotagmin-1 (16–18), we created mutations in the putative Ca^{2+}-binding sites of DOC2b (i.e., C2A [D157N, D163N] and C2B [D297N, D303N]) and designated the product obtained the CIM (Fig. 4*A*). This type of mutant reportedly loses its calcium-dependent phospholipids-targeting capacity (19,20). As shown in Fig. 4*B*, the CIM mutation markedly inhibited insulin-induced DOC2b translocation. Furthermore, CIM-DOC2b also failed to interact with syntaxin-4 in both the in vivo and the in vitro setting (Fig. 4*C–E*). These results raise the possibility that Ca^{2+} binding is essential for insulin-stimulated DOC2b translocation as well as the interaction with syntaxin-4.

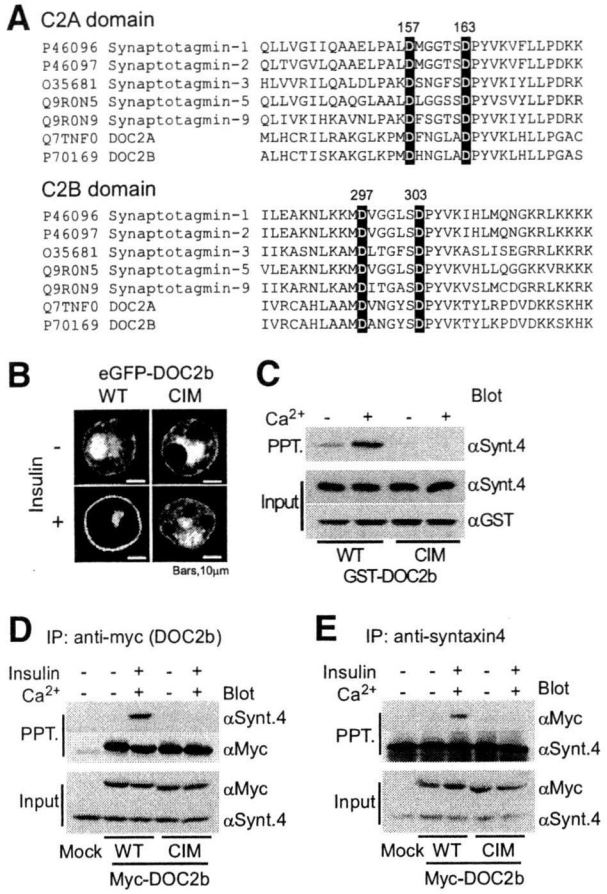

FIG. 4. Calcium binding to DOC2b is essential for its translocation and interaction with syntaxin-4. *A*: ClustalW sequence alignment of C2A and C2B domains from synaptotagmin-1, -2, -3, -5, and -9 and DOC2a and DOC2b. Two aspartic acid residues in each C2 domain (shown on a black background) are well-conserved putative Ca^{2+}-binding sites. These four aspartic acid residues were mutated into asparagine for CIM-DOC2b (D157N, D163N, D297N, and D303N) construction. *B*: Wild-type (WT) or calcium-interacting domain mutants (CIM) of eGFP-DOC2b were expressed in 3T3-L1 adipocytes, which were then treated with insulin and observed under a confocal microscope. Figures show representative images of three independent experiments. *C*: Purified GST-DOC2b (WT or CIM) and syntaxin-4 were mixed in the presence of 2 mmol/l EDTA or 1 mmol/l of $CaCl_2$ and pulled down with glutathione sepharose. The precipitates were analyzed by Western blotting with anti–syntaxin-4 and anti-GST antibodies. *D* and *E*: Myc-tagged DOC2b (WT or CIM) was expressed in 3T3-L1 adipocytes. After serum starvation, the cells were stimulated with or without 100 nmol/l of insulin for 20 min and then immunoprecipitated with anti-myc or anti–syntaxin-4 antibodies. The immunoprecipitated proteins were immunoblotted with anti-myc and anti–syntaxin-4 antibodies.

DOC2b regulates the step of GLUT4 vesicle fusion in response to insulin. One interpretation of the above findings is that DOC2b may act as a Ca^{2+} sensor protein for SNARE complexes triggering GLUT4 vesicle fusion. To assess the role of DOC2b in GLUT4 vesicle fusion to the plasma membrane, we utilized a GLUT4 construct containing four myc epitopes in the first exofacial loop of GLUT4 and an eGFP fusion at its cytoplasmic COOH terminus. These exofacial tags are easily detected by anti-myc antibody but only when GLUT4 vesicles are fused to the plasma membrane (21). Adipocytes expressing this GLUT4 construct and DsRed2-DOC2b (wild type or CIM) or shRNAs were observed by confocal microscopy. As shown in Fig. 5*A* and *B*, the externalized GLUT4 was increased in the cells coexpressing wild-type DOC2b, while being decreased in those coexpressing CIM-DOC2b or shRNA ($shRNA_{DOC2b}$) compared with the control cells. Since the above conclusions were based on qualitative visual impression, we next estimated the fluorescent signals of the cellular rims in Fig. 5*A* and *B* in two ways. First, we counted the number of the cells with eGFP rims (50 cells in each condition) in the cells expressing myc-GLUT4-eGFP. As shown in Fig. 5*C*, just translocated or docked GLUT4 detected by eGFP fluorescence did not change under either condition. Second, we quantified the ratio of cell surface GLUT4 (myc sinal) to GLUT4 translocated to plasma membrane (eGFP signal) as previously described (22). As shown in Fig. 5*D* and *E*, cell surface GLUT4 was increased in the cells expressing wild-type DOC2b but decreased in those expressing CIM-DOC2b and silenced DOC2b (Fig. 5*D* and *E*). These results, taken together with the data shown in Fig. 5*A*, are consistent with the idea that DOC2b is a calcium-sensing protein and regulates the GLUT4 vesicle fusion step in response to insulin.

Role of DOC2b in glucose transport in 3T3-L1 adipocytes. We next focused on the role of DOC2b in insulin-dependent glucose uptake in adipocytes expressing wild-type DOC2b and CIM-DOC2b. As shown in Fig. 6*A*, overexpression of wild-type DOC2b increased insulin-stimulated glucose uptake to 122% of the control level. In contrast, overexpression of CIM-DOC2b decreased to 78% of the control level. Furthermore, we introduced shRNAs ($shRNA_{DOC2b,\ control}$) by adenovirus vectors into cultured adipocytes to induce specific degradation of the DOC2b mRNA. DOC2b protein expression was decreased to 50 and 10% of the control level in the cells infected with viruses at multiplicity of infection (MOI) of 20 and 50, respectively (Fig. 6*B*). As expected, glucose uptake was decreased from 87 to 60% in adipocytes infected with the adenovirus vectors at MOI of 20–50 (Fig. 6*B*). To confirm the specificity of silencing, we conducted add-back style rescue experiment using adenovirus vector containing wild-type DOC2b. As shown in online appendix Fig. S3, overexpression of DOC2b rescued the inhibitory effect on glucose uptake in DOC2b-silenced cells. Under these conditions, DOC2b overexpression and silencing had no effects on serine phosphorylation of Akt (Fig. 6*A* and *B* and online appendix Fig. S3). These results, taken together with the data presented in Figs. 2–5, suggest that DOC2b regulates glucose transport through modulating vesicle fusion processes but not insulin signaling.

DISCUSSION

Regulation of glucose uptake in muscle and adipose tissues by insulin is of fundamental importance for proper maintenance of postprandial hyperglycemia. This hormone stimulates translocation of the GLUT4 glucose transporter from the intracellular membrane to the cell surface (1,2). In addition to this movement of intracellular vesicles containing GLUT4, it has been suggested that the docking and fusion step of GLUT4 vesicles is also critically regulated by insulin (3,4,23). However, the precise mechanism by which insulin regulates vesicle fusion is still largely unknown.

A key finding of this study is identification of the double C2 domain protein DOC2b, which mediates insulin-regulated GLUT4 vesicle fusion. Like other membrane fusion processes, GLUT4 vesicle fusion occurs essentially through the formation of a "core complex" consisting of syntaxin-4 and VAMP-2 (5). In general, however, a number of additional factors are required to bring about SNARE-mediated membrane fusion in vivo. Many of these factors,

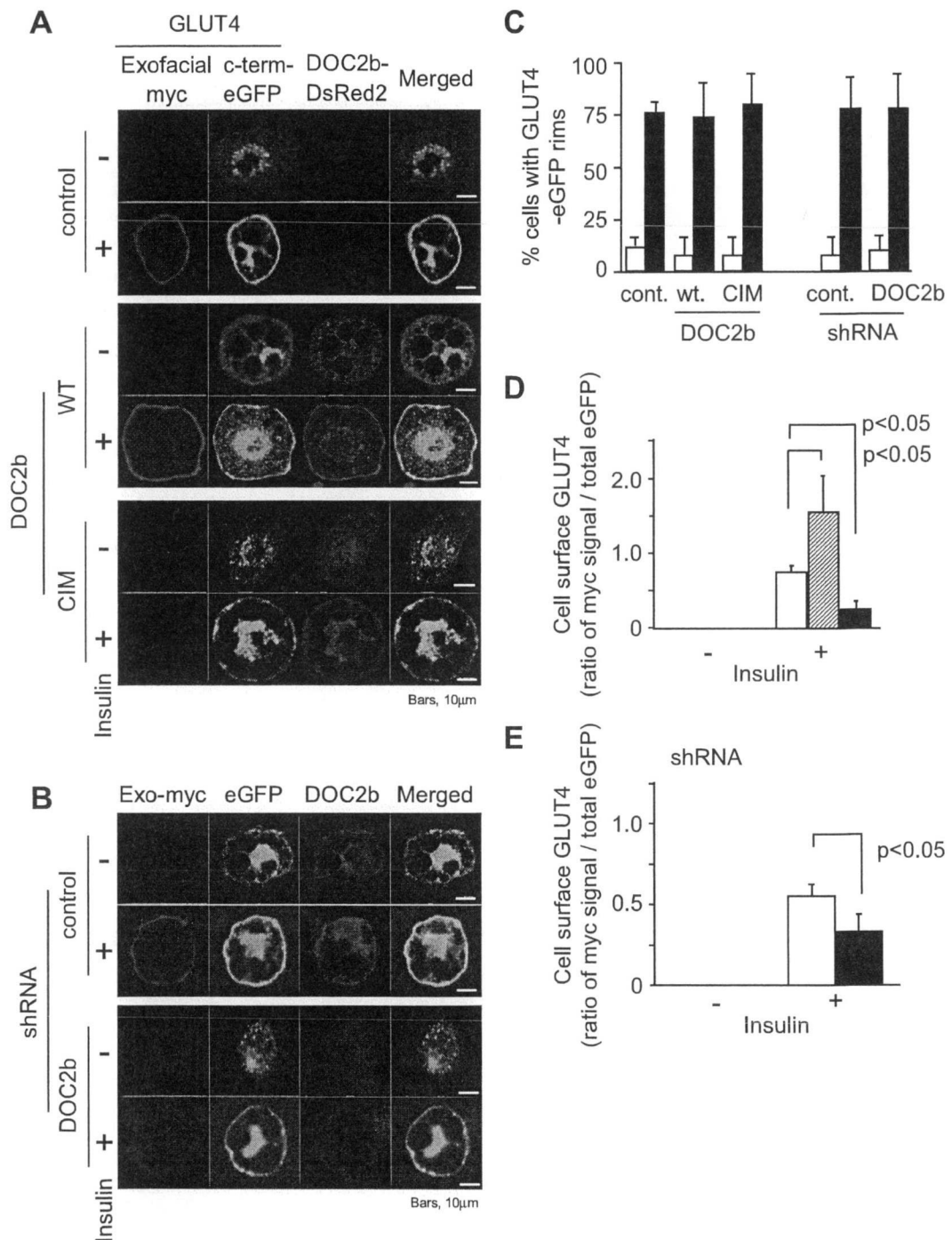

FIG. 5. DOC2b enhances GLUT4 vesicle fusion in 3T3-L1 adipocytes. *A* and *B*: Exofacial myc-tagged GLUT4-eGFP and DsRed2-DOC2b or pcPUR-U6i-shRNA$_{DOC2b,control}$ were coelectroporated into 3T3-L1 adipocytes. The cells were serum starved for 2–4 h and either untreated or treated with 100 nmol/l of insulin for 20 min. The cells were then fixed and stained with anti-myc antibody and Cy5-labeled secondary antibody without detergents. In the cells electroporated with shRNAs, endogenous DOC2b were visualized with anti-DOC2b antibody, followed by Cy3-labeled secondary antibody. Stained cells were observed by confocal microscopy. This shRNA system decreased DOC2b protein expression to 10–20% of control level. Images are representative of three independent experiments. *C–E*: Percents of cells with GLUT4-eGFP rims and the cell surface myc-GLUT4 contents (the ratio of myc signal/eGFP signal at plasma membrane rims) in Fig. 5*A* was calculated as described under RESEARCH DESIGN AND METHODS. *C*: □, −insulin; ■, +insulin. *D*: □, control; ▨, wild type; ■, CIM. E: □, shRNA control; ■, shRNA DOC2b. The graphs represent values from at least 3–5 independent experiments, and error bars show SD. (Please see http://dx.doi.org/10.2337/db08-0303 for a high-quality digital representation of this figure.)

which can collectively be called SNARE regulators (e.g., munc18, synaptotagmin, munc13, GATE-16/Apg8, LMA1, synaptophysin, tomosyn, and Vsm1/Ddi1), bind directly to SNARE proteins and are involved in membrane trafficking and fusion events (24). Among these SNARE regulators, munc18c and tomosyn were reported to be negative regulators of the SNARE complex assembly involved in GLUT4 vesicle fusion (25–27). Despite numerous investigations, the positive SNARE regulators for GLUT4 vesicle fusion have not been adequately clarified. In this report, we have shown that

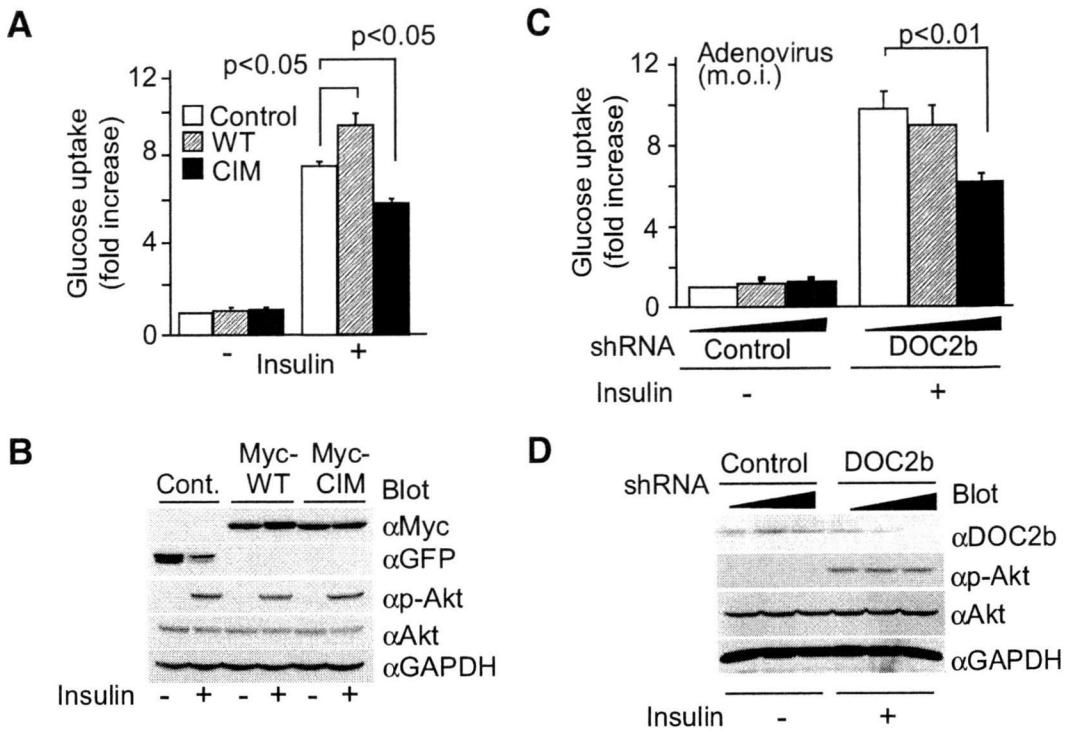

FIG. 6. DOC2b regulates insulin-stimulated glucose uptake in 3T3-L1 adipocytes. 3T3-L1 adipocytes were infected with recombinant adenovirus vectors encoding eGFP, myc-tagged DOC2b (WT, CIM) at MOI of 50 (*A* and *B*) or adenovirus vectors encoding shRNA specific for DOC2b or nontargeting control at MOI of 0, 20, and 50 (*C* and *D*). After serum starvation, the cells were treated with or without 100 nmol/l of insulin for 10 min. *A*: □, control; ▨ wild type;; ■, CIM. *C*: □, 0; ▨, 20; ■, 50. 2-Deoxy-glucose uptake was measured under each condition. Results are presented as means ± SD of at least five independent experiments. *B* and *D*: The cell lysates were also immunoblotted with anti-myc, anti-GFP, anti-DOC2b, anti-Akt, anti–phosphoserine-Akt, and anti–glyceraldehyde-3-phosphate dehydrogenase antibodies. Immunoblots were representative of at least three independent experiments.

DOC2b mediates insulin-stimulated GLUT4 membrane fusion in adipocytes, while having no effect on the GLUT4 vesicle translocation step. These data are consistent with the hypothesis that DOC2b regulates insulin-stimulated GLUT4 vesicle fusion. DOC2b may be a positive SNARE regulator for vesicle fusion processes in adipocytes.

A second significant finding reported herein is the identification of a DOC2b binding partner. DOC2b interacts with t-SNARE syntaxin-4 upon stimulation with insulin in the presence of calcium. Syntaxin-4 is thought to be a SNARE protein on the target membrane for GLUT4 vesicle fusion (28,29). As shown in Fig. 3*A*, this interaction appears to be very strong compared with that between munc18c and syntaxin-4 demonstrated by the yeast two-hybrid method. Although this interaction appeared to be very strong, SNARE proteins are quite sticky and can on occasion bind with many proteins nonspecifically. Therefore, we performed three additional experiments. As shown in Fig. 3*B–E*, we confirmed the interaction between DOC2b and syntaxin-4 in both the in vivo and the in vitro setting. Furthermore, changes in the intracellular localization of DOC2b also supported the functional interaction. As shown in Fig. 2*A*, DOC2b translocates to the plasma membrane in response to insulin stimulation. Importantly, the time scale of DOC2b translocation coincides with relatively slow externalization of GLUT4 vesicles. Taken together, our data are consistent with the aforementioned hypothesis that DOC2b regulates GLUT4 vesicle fusion by triggering SNARE complex assembly.

Another interesting observation made in this study is the essential role of $[Ca^{2+}]i$ in insulin-stimulated GLUT4 vesicle fusion. In 2001, Whitehead et al. (8) first reported that a calcium chelator, BAPTA-AM, inhibited GLUT4 externalization and glucose uptake. However, the precise mechanism underlying calcium-dependent GLUT4 vesicle fusion remains unknown because no studies have as yet focused on Ca^{2+}-sensing proteins in adipocytes. DOC2b is structurally similar to the well-known calcium-sensing SNARE regulator synaptotagmins (Fig. 4*A*). Taking these observations together, we hypothesized that DOC2b is a Ca^{2+}-sensing protein that regulates GLUT4 vesicle fusion in adipocytes. To better assess the role of Ca^{2+} in GLUT4 vesicle fusion, we confirmed the following. First, DOC2b translocation and its binding to syntaxin-4 were shown to be $[Ca^{2+}]i$ dependent. Second, mutations in calcium-binding sites on C2 domains of DOC2b resulted in loss of syntaxin-4 binding, GLUT4 externalization, and glucose uptake. In contrast, we also observed DOC2b–syntaxin-4 binding, without insulin action, in a GST pull-down assay, suggesting that $[Ca^{2+}]i$ is necessary for this interaction in vitro (Fig. 3*B*). In parallel, we also found that insulin initiates the DOC2b translocation to plasma membrane and promotes interaction between DOC2b and syntaxin-4 in the presence of Ca^{2+} ions. Based on the above observations, we propose a simple model whereby insulin regulates SNARE regulator DOC2b, and basal level of $[Ca^{2+}]i$ may act in a constitutive manner to promote DOC2b–syntaxin-4 interaction involved in insulin-stimulated GLUT4 vesicle fusion.

A recent report (30) suggests that DOC2 proteins remove munc18 from syntaxin, thereby regulating core SNARE complex formation. This interpretation is very attractive because munc18c is thought to be a negative regulator of GLUT4 vesicle fusion. Although we have no direct data pertaining to

munc18c, it is possible that munc18c and DOC2b may modulate SNARE assembly in a counterregulatory manner. Very recently, Ke et al. (31) reported that DOC2b bound munc18c, but not syntaxin-4, in pancreatic β-cells. This apparent discrepancy on syntaxin-4 binding may be attributable to the different experimental conditions. They performed most of their experiments using a buffer without calcium (i.e., Nonidet P-40 lysis buffer). Since DOC2b has conserved Ca^{2+}-binding sites and is thought to be a Ca^{2+} sensor protein in other cell types such as neuron (32) and chromaffin cells (33), Ca^{2+} might be important for the physiological properties of DOC2b in β-cells. Further work is required to uncover the underling mechanisms by which DOC2b regulates SNARE assembly in response to insulin.

In summary, we have identified DOC2b as a syntaxin-4 binding protein in adipocytes. This protein regulates GLUT4 vesicle fusion as well as glucose uptake in response to insulin stimulation. We have further revealed that DOC2b requires $[Ca^{2+}]i$ and positively regulates the step of GLUT4 vesicle fusion.

ACKNOWLEDGMENTS

This work was partly supported by grants-in-aid for scientific research from the Ministry of Education, Culture, Sports, Science, and Technology of Japan (to M.E. and Y.T.); from the Takeda Scientific Foundation (to M.E.); and by the Research Grant for Longevity Science (to Y.T.).

No potential conflicts of interest relevant to this article were reported.

We thank Dr. R.R. Duncan for the DOC2a,b constructs, Dr. T. Takuma for the munc18c construct, Dr. K. Taira for the pcPUR+U6i cassette, and Dr. M. Fukuda for the anti-DOC2b antibody. We are also very grateful to Dr. Teruo Nishida for generously supporting us in the experiments using the confocal microscope and to Y. Kora, M. Kaneko, K. Yamada, and S. Ota for their technical supports.

REFERENCES

1. Yang J, Holman, GD: Comparison of GLUT4 and GLUT1 subcellular trafficking in basal and insulin-stimulated 3T3-L1 cells. *J Biol Chem* 268:4600–4603, 1993
2. Czech MP, Corvera S: Signaling mechanisms that regulate glucose transport. *J Biol Chem* 274:1865–1868, 1999
3. Koumanov F, Jin B, Yang J, Holman GD: Insulin signaling meets vesicle traffic of GLUT4 at a plasma-membrane-activated fusion step. *Cell Metab* 2:179–189, 2005
4. Gonzalez E, McGraw TE: Insulin signaling diverges into Akt-dependent and -independent signals to regulate the recruitment/docking and the fusion of GLUT4 vesicles to the plasma membrane. *Mol Biol Cell* 17:4484–4493, 2006
5. Cheatham B, Chuk AV, Kahn CR, Wang L, Rhodes CJ, Klip A: Insulin-stimulated translocation of GLUT4 glucose transporters requires SNARE-complex proteins. *Proc Natl Acad Sci U S A* 93:15169–15173, 1996
6. Burgoyne RD, Morgan A: Secretory granule exocytosis. *Physiol Rev* 83:581–632, 2003
7. Tucker WC, Weber T, Chapman ER: Reconstitution of Ca^{2+}-regulated membrane fusion by synaptotagmin and SNAREs. *Science* 304:435–438, 2004
8. Whitehead JP, Molero JC, Clark S, Meneilly MS, James DE: The role of Ca^{2+} in insulin-stimulated glucose transport in 3T3-L1 cells. *J Biol Chem* 276:27816–27824, 2001
9. Perin MS, Fried VA, Mignery GA, Jahn R, Sudhof TC: Phospholipid binding by a synaptic vesicle protein homologous to the regulatory region of protein kinase C. *Nature* 345:260–263, 1990
10. Rickman C, Craxton M, Osborne S, Davletov B: Comparative analysis of tandem C2 domains from the mammalian synaptotagmin family. *Biochem J* 378:681–686, 2004
11. Miyagishi M, Taira K: U6 promoter-driven siRNAs with four uridine 3′ overhangs efficiently suppress targeted gene expression in mammalian cells. *Nat Biotechnol* 20:497–500, 2002
12. Kuroda TS, Fukuda M: Rab27A-binding protein Slp2-a is required for peripheral melanosome distribution and elongated cell shape in melanocytes. *Nat Cell Biol* 6:1195–1203, 2004
13. Hui E, Bai J, Wang P, Sugimori M, Llinas RR, Chapman ER: Three distinct kinetic groupings of the synaptotagmin family: candidate sensors for rapid and delayed exocytosis. *Proc Natl Acad Sci U S A* 102:5210–5214, 2005
14. Fukuda M, Saegusa C, Kanno E, Mikoshiba K: The C2A domain of double C2 protein γ contains a functional nuclear localization signal. *J Biol Chem* 276:24441–24444, 2001
15. Volchuk A, Wang Q, Ewart HS, Liu Z, He L, Bennett MK, Klip A: Syntaxin 4 in 3T3-L1 adipocytes: regulation by insulin and participation in insulin-dependent glucose transport. *Mol Biol Cell* 7:1075–1082, 1996
16. Sutton RB, Davltov BA, Berghuis AM, Sudhof TC, Sprang S: Structure of the first C2 domain of synaptotagmin I: a novel Ca^{2+}/phospholipid-binding fold. *Cell* 80:929–938, 1995
17. Shao X, Davletov BA, Sutton RB, Sudhof TC, Rizo J: Bipartite Ca^{2+}-binding motif in C2 domains of synaptotagmin and protein kinase C. *Science* 273:248–251, 1996
18. Fernandez I, Arac D, Ubach J, Gerber SH, Shin O, Gao Y, Anderson R, Sudhof TC, Rizo J: Three-dimensional structure of the synaptotagmin 1 C2B-domain: synaptotagmin 1 as a phospholipid binding machine. *Neuron* 32:1057–1069, 2001
19. Fukuda M, Kojima T, Mikoshiba K: Regulation by bivalent cations of phospholipid binding to the C2A domain of synaptotagmin III. *Biochem J* 323:421–425, 1997
20. Mackler JM, Drummond JA, Loewen CA, Robinson IM, Reist NE: The C_2B Ca^{2+}-binding motif of synaptotagmin is required for synaptic transmission in vivo. *Nature* 418:340–344, 2002
21. Bogan JS, McKee AE, Lodish HF: Insulin-responsive compartments containing GLUT4 in 3T3-L1 and CHO cells: regulation by amino acid concentrations. *Mol Cell Biol* 21:4785–4806, 2001
22. Park JG, Bose A, Leszyk J, Czech MP: PYK2 as a mediator of endothelin-1/G alpha 11 signaling to GLUT4 glucose transporters. *J Biol Chem* 276:47751–47754, 2001
23. Lizunov VA, Matsumoto H, Zimmerberg J, Cushman SW, Frolov VA: Insulin stimulates the halting, tethering, and fusion of mobile GLUT4 vesicles in rat adipose cells. *J Cell Biol* 169:481–489, 2005
24. Gerst JE: SNARE regulators: matchmakers and matchbreakers. *Biochim Biophys Acta* 1641:99–110, 2003
25. Thurmond DC, Ceresa BP, Okada S, Elemendorf JS, Coker K, Pessin JE: Regulation of insulin-stimulated GLUT4 translocation by Munc18c in 3T3-L1 adipocytes. *J Biol Chem* 273:33876–33883, 1998
26. Kanda H, Tamori Y, Shinoda H, Yoshikawa M, Sakaue M, Udagawa J, Otani H, Tashiro F, Miyazaki J, Kasuga M: Adipocytes from Munc18c-null mice show increased sensitivity to insulin-stimulated GLUT4 externalization. *J Clin Invest* 115:291–301, 2005
27. Widberg CH, Bryant NJ, Girotti M, Res S, James DE: Tomosyn interacts with the t-SNAREs syntaxin4 and SNAP23 and plays a role in insulin-stimulated GLUT4 translocation. *J Biol Chem* 278:35093–35101, 2003
28. Tellam JT, Macaulay SL, Mcintosh S, Hewish DR, Ward CW, James DE: Characterization of munc-18c and syntaxin-4 in 3T3-L1 adipocytes. *J Biol Chem* 272:6179–6186, 1997
29. Yang C, Coker KJ, Kim JK, Mora S, Thurmond DC, Davis AC, Yang B, Williamson RA, Shulman GI, Pessin JE: Syntaxin 4 heterozygous knockout mice develop muscle insulin resistance. *J Clin Invest* 107:1311–1318, 2001
30. Verhage M, de Vries KJ, Roshol H, Burbach JP, Gispen WH, Sudhof TC: DOC2 proteins in rat brain: complementary distribution and proposed function as vesicular adapter proteins in early stages of secretion. *Neuron* 18:453–461, 1997
31. Ke B, Oh E, Thurmond DC: Doc2beta is a novel munc18c-interacting partner and positive effector of syntaxin 4-mediated exocytosis. *J Biol Chem* 282:21786–21797, 2007
32. Groffen AJ, Friedrich R, Brian EC, Ashery U, Verhage M: DOC2A and DOC2B are sensors for neuronal activity with unique calcium-dependent and kinetic properties. *J Neurochem* 97:818–833, 2006
33. Friedrich R, Groffen AJ, Connell E, van Weering JR, Gutman O, Henis YI, Davletov B, Ashery U: DOC2B acts as a calcium switch and enhances vesicle fusion. *J Neurosci* 28:6794–6806, 2008

Diabetologia (2009) 52:653–663
DOI 10.1007/s00125-009-1270-6

ARTICLE

Increased insulin demand promotes while pioglitazone prevents pancreatic beta cell apoptosis in *Wfs1* knockout mice

M. Akiyama · M. Hatanaka · Y. Ohta · K. Ueda · A. Yanai · Y. Uehara · K. Tanabe · M. Tsuru · M. Miyazaki · S. Saeki · T. Saito · K. Shinoda · Y. Oka · Y. Tanizawa

Received: 7 May 2008 / Accepted: 29 December 2008 / Published online: 4 February 2009

Abstract
Aims/hypothesis The *WFS1* gene encodes an endoplasmic reticulum (ER) membrane-embedded protein called Wolfram syndrome 1 protein, homozygous mutations of which cause selective beta cell loss in humans. The function(s) of this protein and the mechanism by which the mutations of this gene cause beta cell death are still not fully understood. We hypothesised that increased insulin demand as a result of obesity/insulin resistance causes ER stress in pancreatic beta cells, thereby promoting beta cell death.
Methods We studied the effect of breeding *Wfs1*$^{-/-}$ mice on a C57BL/6J background with mild obesity and insulin resistance, by introducing the agouti lethal yellow mutation (*A*^{y}*/a*). We also treated the mice with pioglitazone.
Results *Wfs1*$^{-/-}$ mice bred on a C57BL/6J background rarely develop overt diabetes by 24 weeks of age, showing only mild beta cell loss. However, *Wfs1*$^{-/-}$ *A*^{y}*/a* mice developed selective beta cell loss and severe insulin-deficient diabetes as early as 8 weeks. This beta cell loss was due to apoptosis. In *Wfs1*$^{+/+}$ *A*^{y}*/a* islets, levels of ER chaperone immunoglobulin-binding protein (BiP)/78 kDa glucose-regulated protein (GRP78) and phosphorylation of eukaryotic translation initiation factor 2, subunit α (eIF2α) apparently increased. Levels of both were further increased in *Wfs1*$^{-/-}$ *A*^{y}*/a* murine islets. Electron micrography revealed markedly dilated ERs in *Wfs1*$^{-/-}$ *A*^{y}*/a* murine beta cells. Interestingly, pioglitazone treatment protected beta cells from apoptosis and almost completely prevented diabetes development.

Electronic supplementary material The online version of this article (doi:10.1007/s00125-009-1270-6) contains supplementary material, which is available to authorised users.

M. Akiyama · M. Hatanaka · Y. Ohta · K. Tanabe · M. Tsuru · M. Miyazaki · Y. Tanizawa (✉)
Division of Endocrinology, Metabolism, Hematological Sciences and Therapeutics,
Department of Bio-Signal Analysis,
Yamaguchi University Graduate School of Medicine,
1-1-1 Minami Kogushi,
Ube, Yamaguchi 755-8505, Japan
e-mail: tanizawa@yamaguchi-u.ac.jp

K. Ueda
Health Service Center, Organization for University Education,
Yamaguchi University,
Ube, Yamaguchi, Japan

A. Yanai · K. Shinoda
Division of Neuroanatomy, Department of Neuroscience,
Yamaguchi University Graduate School of Medicine,
Ube, Yamaguchi, Japan

Y. Uehara · S. Saeki · T. Saito
Applied Medical Engineering Science,
Yamaguchi University Graduate School of Medicine,
Ube, Yamaguchi, Japan

K. Tanabe
The Japan Health Science Foundation,
Tokyo, Japan

Y. Oka
Division of Molecular Metabolism and Diabetes,
Department of Internal Medicine,
Tohoku University Graduate School of Medicine,
Sendai, Japan

Conclusions/interpretation *Wfs1*-deficient beta cells are susceptible to ER stress. Increased insulin demand prompts apoptosis in such cells in vivo. Pioglitazone, remarkably, suppresses this process and prevents diabetes. As common *WFS1* gene variants have recently been shown to confer a risk of type 2 diabetes, our findings may be relevant to the gradual but progressive loss of beta cells in type 2 diabetes.

Keywords Apoptosis · Diabetes mellitus · Endoplasmic reticulum · Endoplasmic reticulum stress · Insulin · Pancreatic beta cell · Pioglitazone · Wolfram syndrome

Abbreviations

eIF2α	Eukaryotic translation initiation factor 2,subunit α
ER	Endoplasmic reticulum
GRP78	78 kDa Glucose-regulated protein
GRP94	94 kDa Glucose-regulated protein
ipGTT	Intraperitoneal glucose tolerance test
IRE1	Inositol-requiring protein 1
ITT	Insulin tolerance test
UPR	Unfolded protein response
WFS1	Wolfram syndrome 1
WT	Wild-type

Introduction

Many obese individuals with marked insulin resistance do not develop overt diabetes. However, in individuals destined to develop type 2 diabetes, pancreatic beta cells fail to produce enough insulin to meet systemic demand. This beta cell failure is caused by insufficient beta cell response to glucose and inadequate beta cell mass expansion [1]. Recently, several reports have convincingly confirmed the contribution of beta cell mass reduction to type 2 diabetes [2, 3], at least in its advanced stages. Although the cause of this decrease is unknown, increased apoptosis may play an important role [1, 2]. In addition to genetic factors, processes involving glucotoxicity and/or lipotoxicity are likely to be contributory [4]. Endoplasmic reticulum (ER) stress has also recently emerged as a candidate mechanism [5–7].

Wolfram syndrome is a rare recessively inherited genetic disorder, characterised by juvenile-onset diabetes mellitus and progressive optic atrophy [8]. Several neuro-psychiatric illnesses may also be present [9]. Beta cells are selectively lost from the pancreatic islets and this loss is genetically programmed [10]. Our group and others previously identified the Wolfram syndrome gene, designating it *WFS1* [11] or wolframin [12] and showing that it is localised primarily in the ER [13, 14]. Homozygous *Wfs1* knockout mice developed glucose intolerance. However, the diabetic phenotype of the $Wfs1^{-/-}$ mouse was milder than that seen in Wolfram syndrome patients and was largely dependent on genetic background [15].

Despite intensive studies, the precise function of the Wolfram syndrome 1 (WFS1) protein is still largely unknown. It may regulate ER calcium homeostasis by serving as an ER cation channel [16, 17]. Recently the WFS1 protein was also suggested to be a putative chaperone for the Na/K ATPase b1 subunit in the ER [18]. However, it is certain that its function is closely related to ER stress responses. ER stress induces *Wfs1* expression and, in turn, loss of WFS1 protein exacerbates ER stress [15, 19–21]. Furthermore, $Wfs1^{-/-}$ islet cells are susceptible to ER stress-induced apoptosis [15, 21, 22]. ER stress is induced under conditions such as overload of protein synthesis/processing, accumulation of structurally abnormal proteins, disturbance of post-translational modification and ER calcium homeostasis abnormalities. When ER stress develops, cells respond by unfolded protein response (UPR), facilitating protein folding via the induction of chaperone proteins, attenuation of translations, as well as degradation of misfolded proteins, a process called ER-associated degradation [23–25]. If the stress is severe, apoptosis is induced. Accumulating evidence suggests that a high level of ER stress or defective ER stress signalling causes beta cell death and that diabetes thereby develops [26–30].

We wished to test in vivo the hypothesis that beta cell loss in $Wfs1^{-/-}$ mice is caused by an inability to cope with ER stress. The agouti yellow (A^y/a) mouse is a genetic model of mild obesity/insulin resistance with compensatory beta cell hyperplasia [31]. In this mouse, ectopically expressed agouti protein promotes food intake and weight gain by antagonising signalling at melanocortin-4 receptor in the hypothalamus. ER stress is likely to have been induced in these beta cells by increased insulin synthesis and secretion demands, and also by elevated serum NEFA [32]. As $Wfs1^{-/-}$ mice on the C57BL/6J background rarely develop overt diabetes by 24 weeks, we introduced the A^y mutation into C57BL/6J $Wfs1^{-/-}$ mice and assessed the consequences. Furthermore, we treated $Wfs1^{-/-}$ mice with pioglitazone, which ameliorates insulin resistance.

Methods

Animals All experimental protocols were approved by the Ethics of Animal Experimentation Committee at Yamaguchi University School of Medicine.

The $Wfs1^{-/-}$ mice had a C57BL/6J background [15]. The Agouti yellow mice (C57BL/6J*HamSlc-A^y*) were obtained from M. Nishimura (Nagoya University Graduate School of Medicine, Nagoya, Japan) and Japan SLC

(Hamamatsu, Japan). We used male mice for all experiments. The mice were kept under standard, specific pathogen-free conditions with a constant dark/light cycle and free access to standard mouse chow (MF; Oriental Yeast, Tokyo, Japan) and water. The high-fat diet (rodent diet with 60% energy from fat; D12492) was purchased from Research Diet (New Brunswick, NJ, USA) and was freely accessible. For pioglitazone treatment, mice were fed standard mouse chow with 0.01% pioglitazone (wt/wt) from the age of 4 weeks. Pioglitazone was provided by Takeda Pharmaceutical (Osaka, Japan).

Generation of $Wfs1^{-/-}$ A^y/a mice To generate A^y/a mice lacking the *Wfs1* gene, $Wfs1^{-/-}$ mice were bred with A^y/a mice to create the compound heterozygote ($Wfs1^{+/-}$ A^y/a). This heterozygote was bred with $Wfs1^{+/-}$ a/a, and $Wfs1^{-/-}$ A^y/a, $Wfs1^{+/+}$ A^y/a, $Wfs1^{-/-}$ a/a and $Wfs1^{+/+}$ a/a (wild-type [WT]) offspring were identified.

The *Wfs1* genotype was determined by PCR. We used the sense primer 5′-CCCAGTTCTTGCTTTACCAC CAGG-3′ and the anti-sense primers 5′-GCCTTCTTGAC GAGTTCTTCTGA-3′ (derived from the neomycin resistance gene) and 5′-ACTTCGTCCAGCACTGGGGTCAG-3′ (derived from the *Wfs1* gene). A^y/a mice were identified by coat colour.

Physiological studies Body weights were measured weekly. Blood samples were collected from the tail vein. Non-fasting blood glucose was measured by the glucose oxidase method using a GlucoCard device (Arkray, Kyoto, Japan). Serum insulin levels were determined using an insulin ELISA kit (Morinaga Institute of Biological Science, Tokyo, Japan). Serum triacylglycerol was measured by high-performance liquid chromatography at Skylight Biotech (Akita, Japan), according to the procedure described by Usui et al. [33]. Intraperitoneal glucose tolerance test (ipGTT) and insulin tolerance test (ITT) were performed at 8 weeks of age.

Pancreatic insulin content Pancreases were removed and homogenised in acid/ethanol (0.7 mol/l HCl/ethanol 25:75 plus 0.1% Triton X-100 (vol./vol.)) and left at 4°C for 48 h, with sonication every 24 h. Homogenates were then centrifuged (3,000 *g* for 15 min) and the insulin content of the acid/ethanol supernatant fraction was measured using insulin ELISA. Protein in tissue extracts was determined using the BCA protein assay reagent.

Immunostaining and morphometry Formalin-fixed paraffin-embedded sections were de-paraffinised and re-hydrated, then incubated with primary antibodies. For immunofluorescent staining, appropriate FITC-conjugated or Cy3-conjugated anti-IgG was used. Detailed antibody information is given in the Electronic supplementary material (ESM). Immunohistochemical analyses were performed, with at least three animals for each condition being killed for the purpose. For measurement of beta cell area, more than five pancreatic tissue sections per animal were randomly selected and stained with anti-insulin IgG/3,3′-diaminobenzidine tetrahydrochloride and haematoxylin. Microscopic photoimages were taken with a charge-coupled device (CCD) camera and the pancreatic and beta cell areas were each estimated using a computer program (Y. Uehara, S. Saeki and S. Saito S unpublished results).

Tissue preparation and electron microscopy All animals were anaesthetised with sodium pentobarbital (65 mg/kg, i.p.) and intracardially perfused with 2% glutaraldehyde (vol./vol.) and 4% paraformaldehyde (vol./vol.) in 0.1 mol/l phosphate buffer (pH 7.4) containing 0.2% picric acid (vol./vol.). Pancreatic sections (1 mm thick) were post-fixed with 1% OsO_4 (wt/vol.), block-stained with 2% uranyl acetate (wt/vol.), dehydrated, infiltrated with propylene oxide, placed in a mixture of propylene oxide and Epoxy resin (1:1), and flat-embedded on siliconised glass slides in Epoxy resin. Ultrathin sections were made and mounted on to copper grids. To enhance contrast, they were double stained with 2% uranyl acetate (wt/vol.) and 1% lead citrate (wt/vol.), and observed with a Hitachi H-7500 electron microscope (Hitachi High-Technologies, Tokyo, Japan) operating at 80 kV.

Mouse islet isolation and immunoblotting analysis Pancreatic islets were isolated as described previously [15]. For immunoblotting [34], approximately 100 islets from two to six mice were pooled, then immediately dissolved in lysis buffer containing 1% SDS (50 mmol/l Tris–HCl [pH 6.8], 1% SDS [wt/vol.], 10% glycerol [wt/vol.] and 50 mmol/l dithiothreitol). Anti-WFS1 (N-terminus) antibody has been described previously [15]. For information on other antibodies, see ESM.

Statistical analysis Results are expressed as means±SE. Differences between means were evaluated using ANOVA or Student's *t* test as appropriate. Differences were considered significant at $p<0.05$.

Results

Characteristics of the mice Body weights were monitored weekly beginning at 4 weeks of age. A^y/a mice ($Wfs1^{+/+}$ A^y/a) were mildly, but significantly more obese than WT littermates ($Wfs1^{+/+}$ a/a) by 6 weeks of age (23.5±0.7 vs 21.5± 0.5 g; $p<0.05$). Similarly, $Wfs1^{-/-}$ A^y/a mice were also more obese than $Wfs1^{-/-}$ a/a mice by 6 weeks of age (23.9±0.3 vs 20.6±0.2 g; $p<0.0001$). However, $Wfs1^{-/-}$ A^y/a mice had